Pro Gradu

Implementing the 3-Omega Technique for Thermal Conductivity Measurements

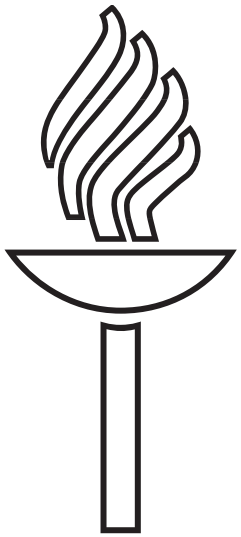

Tuomas Hänninen

April 2013

UNIVERSITY OF JYVÄSKYLÄ
NANOSCIENCE CENTER
DEPARTMENT OF PHYSICS
NANOPHYSICS
SUPERVISOR: ILARI MAASILTA

Abstract

Thermal conductivity of the constituent materials is one of the most important properties affecting the performance of micro- and nanofabricated devices. These devices often make use of thin films with thicknesses ranging from some nanometers to few micrometers. The thermal conductivity of thin films can be measured with the three-omega method. In three-omega technique a metal wire acting as a resistive heater is microfabricated on the sample. Alternating current passing through the metal heater at a frequency ω heats the sample periodically and generates oscillations in the resistance of the metal line at a frequency 2ω. The oscillating resistance component is coupled with the driving current to create a third harmonic (3ω) voltage component over the heater. The magnitude and frequency dependence of the 3ω voltage can be used to obtain the thermal properties of the sample.

The measurement setup consisted of a vacuum chamber with a custom sample mount, lock-in amplifiers to supply the voltage and to record the output, and various other electrical components. Custom LabVIEW programs were used for data-acquisition and input signal modification.

The goal of the project was to build and validate a 3ω-measurement setup by measuring the thermal conductivities of 300 nm thick SiO_2 thin films. Bismuth and gold were used as the heater materials because they have noticeable temperature coeffcients of resistivity, bismuth even at temperatures of a few kelvin. Data analysis revealed that the output of the examined measurement setups can not be used to calculate the thermal properties of the samples. This is most probably due to spurious 3ω-signal in the measurement circuit, originating from the components and voltage sources.

Tiivistelmä

Valmistusaineiden lämmönjohtavuus on yksi tärkeimmistä mikro- ja nanovalmistettujen laitteiden toimintaan vaikuttavista ominaisuuksista. Usein näissä laitteissa materiaaleja käytetään ohuina kerroksina tai kalvoina, joiden paksuus voi vaihdella muutamista nanometreistä muutamiin mikrometreihin. Ohutkalvojen lämmönjohtavuutta voidaan mitata kolme-omega-menetelmällä. Kolme-omega-menetelmässä näytteen pinnalle valmistettu metallijohdin toimii resistiivisenä lämmittimenä. Metallilämmittimen läpi taajuudella ω kulkeva vaihtovirta lämmittää metallia jaksollisesti ja aiheuttaa oskillaatioita metallilangan resistanssissa taajuudella 2ω. Oskilloiva resistanssikomponentti yhdessä langan läpi kulkevan virran kanssa aiheuttaa 3ω-taajuisen jännitekomponentin langan päiden välille. Tämän 3ω-jännitteen suuruutta ja taajuusriippuvuutta voidaan käyttää näytteen termisten ominaisuuksien määrittämiseen.

Mittausjärjestely koostui tyhjiökammiosta ja räätälöidystä näytealustasta, tarvittavista sähköisistä komponenteista ja lukitusvahvistimista, joilla syötettiin piiriin vaihtojännite ja mitattiin saatu ulostulosignaali. Datankeruu ja syöttösignaalin ohjaus suoritettiin erityisillä LabVIEW-ohjelmilla.

Projektin tarkoituksena oli rakentaa ja validoida kolme-omega-mittausjärjestely mittaamalla 300 nanometriä paksujen piidioksidikalvojen lämmönjohtavuuksia. Vismuttia ja kultaa kokeiltiin lämmitinlangan materiaalina, koska niillä on huomattava resistiivisyyden lämpötilavaste, vismutilla aina muutaman kelvinin lämpötiloihin asti. Data-analyysi paljasti, että saatua mittausdataa ei voida käyttää näytteiden lämpöominaisuuksien määrittämiseen. Syy tälle on todennäköisesti mittauspiiristä ja signaalilähteistä aiheutuva häiriösignaali.

Contents

1 Introduction

Thin films are routinely used in microfabricated devices in electronics and micromechanical applications. The thickness of the film can be as low as a couple of nanometers, it can be crystalline or amorphous, it can be suspended or a piece in a multilayer stack, and its purpose can be anything from a wear-resistant coating to a conductive layer. Along electrical, optical, and mechanical properties, thermal properties are a major factor affecting the performance of the devices. Often the operational temperature range of devices can range even hundreds of degrees or the operational temperatures are extremely high or low. Because of the low height dimension, the thermal conductivity of the thin film can differ drastically from the bulk material value. These factors result in a need to identify the thermal properties, most importantly the thermal conductivity, of films precisely over a wide temperature regime.

The thermal conductivity of the sample can be defined either by a steady-state or a time-dependent (transient) method. Steady-state thermal conductivity measurement methods require long equilibration times, are prone to radiation errors, and are not suitable for film-like specimens as multiple contacts into the sample are required to extract the relevant data. Transient techniques generally require only a single contact into the surface of the sample and are remarkably faster than the steady-state methods. Two transient methods have been used extensively for measuring thermal conductivity of thin films, time-domain thermoreflectance (TDTR) and the three-omega method [1, 2].

Time-domain thermoreflectance utilizes a femtosecond or picosecond pulsed laser to probe the sample. A "pump" beam is used to heat up a spot on the sample surface and the cooling is monitored by the reflectivity of the low-energy "probe" beam. The sample should be metallic or coated with a thin metal layer, and the change in temperature affects the reflectivity of the metal film and the obtained cooling curve is then compared into theoretical model. The fine resolution of TDTR makes it possible to distinguish the thermal conductance of interfaces from the thermal conductivity of the films. The cost of a picosecond laser equipment makes the method quite expensive and limits its availability. [1, 2]

For electrically insulating materials the three omega method provides an affordable thermal conductivity measurement over a wide temperature range [3]. It is based on the detection of a small third-harmonic voltage

that is created while passing an alternating current through a heater. The third harmonic generation in a metal heater was first observed in the 1910's [4]. At first the method was used to probe the thermal diffusivity of metal filaments used in light bulbs [5]. During the 1960's the technique was used to determine properties like the specific heat of the materials used as heaters in the experiment [6, 7, 8]. In the 1980's a planar heater was used to probe the frequency dependent specific heat of liquids near the glass-transition [9, 10].

The major breakthrough happened in the late 1980's when a thin line heater deposited on the surface of the material of interest was used for the first time [11]. An alternating current is passed through the heater at a frequency ω, resistive heating generates an oscillating resistance component at frequency 2ω. When the oscillating resistance component is coupled with the driving current the result is a small 3ω voltage over the heater. Thermal conductivity of the specimen can be calculated from the frequency dependence of the oscillation amplitude and the phase of the 3ω voltage. Heat affected region of the sample is reduced compared to steady-state methods and the temperature oscillations in the specimen reach dynamic equilibrium after few oscillation cycles. Applicable temperature range for the 3ω method runs from 30 K to 1000 K, depending on the thermal properties of the substrate and the heater geometry [3, 12]. The technique has been used to measure the thermal conductivity of various different materials, including dielectrics [3], porous materials [13], and even carbon nanotubes [14].

2 Theoretical Considerations for 3ω method

In the 3ω method a thin metal line is deposited on the specimen. The metal line acts both as a heater and a resistance thermometer detector (RTD). Alternating current (ac) is used in 3ω measurements because direct current measurements require long equilibration times and are vulnerable to radiation losses. The heater is assumed to be in intimate thermal contact with specimen and its heat capacity is neglected, i.e., the heater is assumed to be massless and/or infinitely good thermal conductor. A typical geometry of the heater/thermometer, used also in this work, is shown in figure 1. [3, 11]

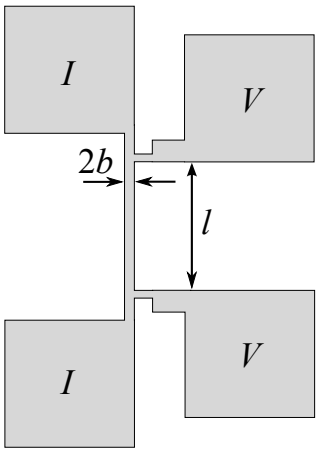

Figure 1: The geometry of the heater/thermometer used in the experiment. The width of the line is $2b$ and the length l. Two bonding pads for both the current input and the voltage readout.

When an ac current is passed through the heater, the power dissipated by the heater due to resistive heating is

$$P = RI^2, \tag{1}$$

where R is the heater resistance and I is the current passing through the heater. The alternating current is of the form

$$I = I_0 \cos(\omega t). \tag{2}$$

Here I_0 is the peak amplitude of the nominal heater current. Now the power can be written as

$$P(t) = \frac{1}{2} I_0^2 R_0 \left(1 + \cos(2\omega t)\right) = P_0 + P_0 \cos(2\omega t), \tag{3}$$

where R_0 is the nominal heater resistance and $P_0 = \frac{1}{2} I_0^2 R_0$. As it is seen in equation (3), the power has a constant component independent of time and an oscillating component. For a sinusoidal current, the rms ac power dissipated over one cycle can be defined as

$$P_{rms} = \frac{1}{2} I_0^2 R_0, \tag{4}$$

which equals P_0.

For small temperature changes the response of the RTD can be written as

$$R = R_0(1 + \beta \Delta T), \tag{5}$$

where β is the temperature coefficient of resistance (TCR), and R_0 and R are the resistances of the metal line at temperatures T_0 and $T_0 + \Delta T$, respectively.

2.1 Fourier's law and the heat diffusion equation

The Fourier's law states that the heat flux, i.e., the flow rate of heat energy through a surface is proportional to the negative temperature gradient across the surface [15]:

$$\vec{\phi} = -k \nabla T, \tag{6}$$

where $\vec{\phi}$ is the heat flux (W/m^2), k is the thermal conductivity of the medium (W/m·K), and ∇T is the temperature gradient in the specimen. In one dimensional system the temperature gradient can be written simply as a spatial derivative of the temperature, and the heat flux is then:

$$\phi = -k \frac{\partial T}{\partial x}. \tag{7}$$

The internal energy of the material per unit volume is related to the temperature by

$$Q = \rho c_p T, \tag{8}$$

where ρ is the mass density of the material (kg/m^3) and c_p is the specific heat capacity (J/kg·K).

The change in the internal energy in a differential spatial region

$$x - \Delta x < \xi < x + \Delta x$$

over a differential time period

$$t - \Delta t < \tau < t + \Delta t$$

can be found by setting

$$c_p \rho \int_{x-\Delta x}^{x+\Delta x} [T(\xi, t + \Delta t) - T(\xi, t - \Delta t)] \, \mathrm{d}\xi = c_p \rho \int_{t-\Delta t}^{t+\Delta t} \int_{x-\Delta x}^{x+\Delta x} \frac{\partial T}{\partial \tau} \, \mathrm{d}\xi \mathrm{d}\tau. \tag{9}$$

If no work is done on or by the the specimen and there are no heat sinks or sources, all the change in the internal energy is due to heat flux across the boundaries. This can be expressed with the Fourier's law as

$$k \int_{t-\Delta t}^{t+\Delta t} \left[\frac{\partial T}{\partial x}(x + \Delta x, \tau) - \frac{\partial T}{\partial x}(x - \Delta x, \tau) \right] \mathrm{d}\tau = k \int_{t-\Delta t}^{t+\Delta t} \int_{x-\Delta x}^{x+\Delta x} \frac{\partial^2 T}{\partial x^2} \, \mathrm{d}\xi \mathrm{d}\tau. \tag{10}$$

These integrals are different expressions for the same thing, the change in the internal energy of the specimen. Due to conservation of energy these must be equal and we can set

$$\int_{t-\Delta t}^{t+\Delta t} \int_{x-\Delta x}^{x+\Delta x} [c_p \rho \frac{\partial T}{\partial \tau} - k \frac{\partial^2 T}{\partial \xi^2}] \, \mathrm{d}\xi \mathrm{d}\tau = 0. \tag{11}$$

For the integral to vanish it must hold that

$$\frac{\partial T}{\partial t} = \frac{k}{\rho c_p} \left(\frac{\partial^2 T}{\partial x^2} \right), \tag{12}$$

which is the heat diffusion equation for a one dimensional system. The coefficient $k/\rho c_p$ is α, the thermal diffusivity and its unit is m^2/s.

2.2 Heat diffusion into specimen from an infinite planar heater with sinusoidal heating

The sinusoidal current with frequency ω passing through the heater results in a steady dc temperature rise and an oscillating ac temperature component [16]. The dc component creates a constant temperature gradient into the specimen while the ac part results in thermal waves diffusing into the specimen at frequency 2ω. To write the ac temperature rise and its effect on the heater resistance, we need to solve the heat diffusion equation for the case of thin infinite planar heater on the surface of the specimen. The system is visualized in figure 2.

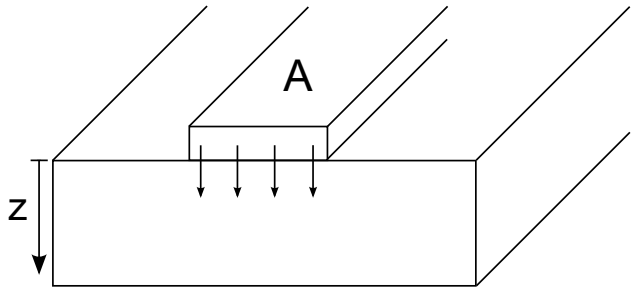

Figure 2: One dimensional heat flow from a thin infinitely long plane heater on a substrate. Heat enters the specimen uniformly over the width of the heater and edge-effects are not considered. The zero level of z-coordinate is located at the heater/specimen interface.

The heat generated in the heater diffuses into the specimen along the positive z-axis, perpendicular to the plane of the heater. Oscillating temperature inside the specimen is dependent both on the distance from the heater and time, and can be written as

$$T = T(z, t). \tag{13}$$

The heat diffusion equation (12) for the system then reads

$$\frac{\rho c_p}{k} \frac{\mathrm{d}T(z,t)}{\mathrm{d}t} - \frac{\mathrm{d}^2 T(z,t)}{\mathrm{d}z^2} = 0. \tag{14}$$

In the case of sinusoidal heating the temperature can be separated into time and spatially dependent parts [15]:

$$T(z, t) = T_z \exp(\mathrm{i}2\omega t). \tag{15}$$

Plugging this into the heat equation, carrying out the differentiation with respect to t and dividing by $\exp(\mathrm{i}2\omega t)$ yields

$$\frac{\mathrm{d}^2 T_z}{\mathrm{d}z^2} - \mathrm{i}\frac{2\omega}{\alpha} T_z = 0\,, \tag{16}$$

where α is the thermal diffusivity, dimensions m^2/s. Solution to the spatial part inside the specimen, where $z > 0$, is

$$T_z = T_0 \exp(-qz), \tag{17}$$

where q is the wavenumber of the thermal wave, defined as

$$q = \sqrt{\mathrm{i}2\omega/\alpha} = (1+\mathrm{i})\sqrt{\frac{\omega}{\alpha}} = \sqrt{\frac{2\omega}{\alpha}} \cdot \exp(\mathrm{i}\pi/4). \tag{18}$$

Solution (17) vanishes at large z and yields the temperature of the heater T_0 at $z = 0$. Now the time dependent periodic temperature inside the specimen can be expressed as

$$T(z,t) = T_0 \exp(\mathrm{i}2\omega t - qz). \tag{19}$$

The heat flux into the specimen right at the heater/sample interface can be written as [17]

$$\begin{aligned} \phi\big|_{z=0^+} &= -k \left.\frac{\mathrm{d}T(z,t)}{\mathrm{d}z}\right|_{z=0^+} = kqT_0 \exp(\mathrm{i}2\omega t) \\ &= kT_0\sqrt{2\omega/\alpha} \cdot \exp(\mathrm{i}2\omega t + \mathrm{i}\pi/4). \end{aligned} \tag{20}$$

The flux equals the oscillating heat component produced in the heater per unit area. The oscillating power component of the heater is seen in equation (3). The oscillating power of the heater can be written in complex notation:

$$P_0 \cos(2\omega t) = P_0 \Re\left(\exp(\mathrm{i}2\omega t)\right). \tag{21}$$

Dividing the complex power by the heater area A and setting it equal to the heat flux from equation (20) gives

$$\frac{P_0}{A} \exp(\mathrm{i}2\omega t) = kT_0\sqrt{2\omega/\alpha}\exp(\mathrm{i}2\omega t + \mathrm{i}\pi/4). \tag{22}$$

This yields us an expression for T_0, the oscillative heater temperature:

$$T_0 = \frac{P_0}{k\sqrt{2\omega/\alpha}A} \cdot \exp(-\mathrm{i}\pi/4) = \frac{P_0}{\sqrt{2\omega c_p k}A} \cdot \exp(-\mathrm{i}\pi/4). \tag{23}$$

Now we can express the specimen temperature oscillations with explicit ω-dependence:

$$T(z,t) = T_0 \exp(\mathrm{i}2\omega t - qz) = \frac{P_0}{\sqrt{2\omega c_p k}A} \cdot \exp(\mathrm{i}2\omega t - \mathrm{i}\pi/4 - qz). \tag{24}$$

Temperature lags the heater current by $\pi/4$ and has $\omega^{-1/2}$-dependence.

Now we can calculate the effect of the oscillative heater temperature to the heater resistance by using equation (5) and the real part of (24) just below the heater where $z = 0$.

$$R(t) = R_0(1 + \beta\Delta T_{dc} + \beta\Delta T_{ac}\cos(2\omega t + \pi/4)), \tag{25}$$

where ΔT_{dc} is the dc temperature rise and ΔT_{ac} is $P_0/A \cdot (2\omega c_p k)^{-1/2}$, the peak amplitude of the ac temperature oscillations. The voltage across the RTD can be obtained by multiplying the heater resistance with the input current, resulting in

$$\begin{aligned} V(t) = I_0 R_0 \Big(&(1 + \beta\Delta T_{dc})\cos(\omega t) + \frac{1}{2}\beta\Delta T_{ac}\cos(\omega t + \pi/4) \\ &+ \frac{1}{2}\beta\Delta T_{ac}\cos(3\omega t + \pi/4)\Big). \end{aligned} \tag{26}$$

The 3ω and ω components in the voltage with phase shift result from multiplying the 2ω term in the resistance with the input current oscillating at the frequency ω. We can express the 3ω amplitude as

$$V_{3\omega} = \frac{1}{2}V_0\beta\Delta T_{ac}, \tag{27}$$

where $V_0 = I_0 R_0$. By measuring the voltage at the frequency 3ω one is able to deduce the in-phase and out-of-phase components of the temperature oscillations.

The finite thermal diffusion time τ_D of the specimen affects both the magnitude and the phase of the temperature oscillations. Required time

for the thermal wave to propagate a distance L in the specimen is given by equation

$$\tau_D = L^2/\alpha\,, \tag{28}$$

where α is the thermal diffusivity [18]. The angular frequency related to the thermal diffusion is directly proportional to thermal diffusivity

$$\omega_D = \frac{2\pi}{\tau_D} = \frac{2\pi\alpha}{l^2} \propto \alpha. \tag{29}$$

If the thermal diffusivity is infinite, no temperature gradients will form into the specimen and there would be no phase lag between the driving current and the temperature oscillations. At the limit of zero thermal diffusivity there would be no heat propagation into the sample.

2.3 One-dimensional line heater inside the specimen

To calculate the thermal conductivity of the material under a line heater, one can first study the simplified model of temperature oscillations a distance $r = (x^2 + y^2)^{1/2}$ away from an infinitely narrow line source of heat on the surface of an infinite half-volume.

First the form of the temperature oscillations has to be solved for the case of infinite volume. The solution can be found in for example Carslaw and Jaeger [15] and their arguments are repeated here. Picture of the arrangement of the infinite case is shown in figure 3. Assuming that there is no axial or circumferential temperature gradients, the spatial heat diffusion equation for the temperature in the cylinder, $T(r,t)$, can be written as

$$\frac{\partial^2 T(r,t)}{\partial r^2} + \frac{1}{r}\frac{\partial T(r,t)}{\partial r} - \frac{1}{\alpha}\frac{\partial T(r,t)}{\partial t} = 0. \tag{30}$$

The temperature function can be divided into spatial and time dependent parts because the heating power is sinusoidal, as was the case for the cartesian system in the previous subsection.

$$T(r,t) = T_r \exp(\mathrm{i}2\omega t). \tag{31}$$

As previously, plugging this into the heat equation, carrying out the differentiation with respect to t and dividing by $\exp(\mathrm{i}2\omega t)$ yields

$$\frac{\mathrm{d}^2 T_r}{\mathrm{d}r^2} + \frac{1}{r}\frac{\mathrm{d}T_r}{\mathrm{d}r} - \mathrm{i}\frac{2\omega}{\alpha}T_r = 0. \tag{32}$$

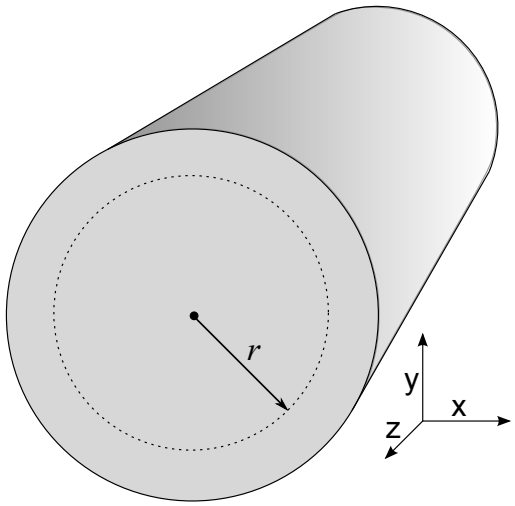

Figure 3: The geometry of an infinite circular cylinder with one dimensional line heater running through the cylinder axis.

Here i2ω/α equals q^2, the wavenumber of the thermal wave squared, found in the previous subsection. Changing variables from r to $y = qr$ yields

$$y^2 \frac{\mathrm{d}^2 T(y)}{\mathrm{d}y^2} + y \frac{\mathrm{d}T(y)}{\mathrm{d}y} - y^2 T(y) = 0. \tag{33}$$

This is a modified Bessel equation of zeroth order. The solution is a linear combination of modified Bessel functions of first and second kind

$$T_r = AI_0(qr) + BK_0(qr), \tag{34}$$

where A and B are constants and $I_0(qr)$ and $K_0(qr)$ are zeroth order modified Bessel functions of first and second kind with arguments qr, respectively. The functions behave oppositely, I_0 grows exponentially and K_0 decays exponentially when increasing the argument, the behavior is shown in figure 4.

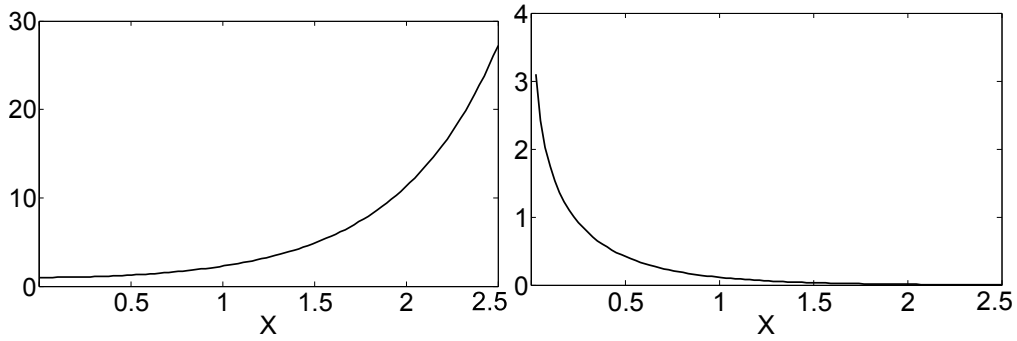

(a) $I_0(x)$. (b) $K_0(x)$.

Figure 4: The behavior of the zeroth order modified Bessel functions of first and second kind when going along the positive x-axis. The function of first kind I_0 explodes, whereas the function of the second kind K_0 decays rapidly.

The coefficient A has to be zero because the temperature should decrease when going away from the heater. Coefficient B can be found by requiring the heat flux through a cylindrical surface at a distance $r = r_0$, where $r_0 \to 0$ away from the heater to match the flux from the line source. From the

Fourier's equation (7):

$$\begin{aligned}\phi\Big|_{r=r_0} &= -k\left.\frac{\mathrm{d}T(r,t)}{\mathrm{d}r}\right|_{r=r_0} = -kB\left.\frac{\mathrm{d}K_0(qr)}{\mathrm{d}r}\right|_{r=r_0}\cdot\exp(\mathrm{i}2\omega t)\\ &= kqBK_1(qr_0)\cdot\exp(\mathrm{i}2\omega t),\end{aligned} \tag{35}$$

where K_1 is a first order modified Bessel function of second kind. On the other hand, the heat flux from the heater through a cylindrical surface at $r = r_0$ is

$$\phi\Big|_{r=r_0} = P/A = \frac{P_0}{2\pi l_{cyl} r_0}\cdot\exp(\mathrm{i}2\omega t). \tag{36}$$

Equaling these we get the coefficient B:

$$B = \frac{P_0}{2k\pi l_{cyl} r_0}\frac{1}{qK_1(qr_0)}. \tag{37}$$

Series expansion for $qr_0K_1(qr_0)$ at $r_0 = 0$ yields

$$qr_0K_1(qr_0) = 1 + O(r_0^2). \tag{38}$$

This gives the expression for the spatial part of the temperature oscillations:

$$T(r) = \frac{P_0}{2k\pi l_{cyl}}K_0(qr). \tag{39}$$

The total function for the temperature in the cylinder is then

$$T(r,t) = \frac{P_0}{2k\pi l_{cyl}}K_0(qr)\cdot\exp(\mathrm{i}2\omega t). \tag{40}$$

2.4 One-dimensional line heater at the surface of the specimen

The result for infinite volume can used to express the temperature oscillations for infinite half-volume. Halving the volume means that twice as much of heat flux flows into the remaining volume, assuming no radiation, convection or conduction on the surface. This is the case for the 3ω method because measurements are done in vacuum and radiation losses are low

due to the rapid decay of the temperature oscillations [3]. Half-infinite case is seen in figure 5. Equation (39) then becomes

$$T(r) = \frac{p_0}{\pi k} K_0(qr), \tag{41}$$

and the total temperature function (40)

$$T(r,t) = \frac{p_0}{\pi k} K_0(qr) \cdot \exp(\mathrm{i}2\omega t), \tag{42}$$

where p_0 equals P_0/l_{cyl}, the heater power per unit length. The real part of the temperature function is visualized in figure 6.

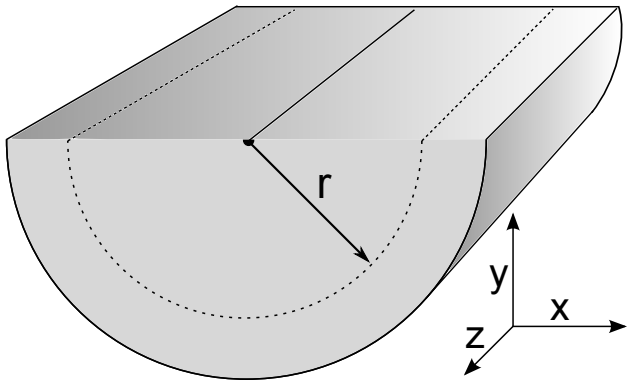

Figure 5: The geometry of a half-infinite circular cylinder with one dimensional line heater at the surface.

Even though the thermal oscillations decay rapidly because of the $K_0(qr)$, one has to make sure that the oscillations are contained inside the sample. This is done by calculating the penetration depth of the thermal wave in the specimen. The thermal penetration depth λ relates to the wavenumber of the thermal wave q by

$$\lambda = \frac{1}{|q|} = \sqrt{\frac{\alpha}{2\omega}}. \tag{43}$$

Specimen can be considered semi-infinite if its thickness exceeds 5 thermal penetration depths [3].

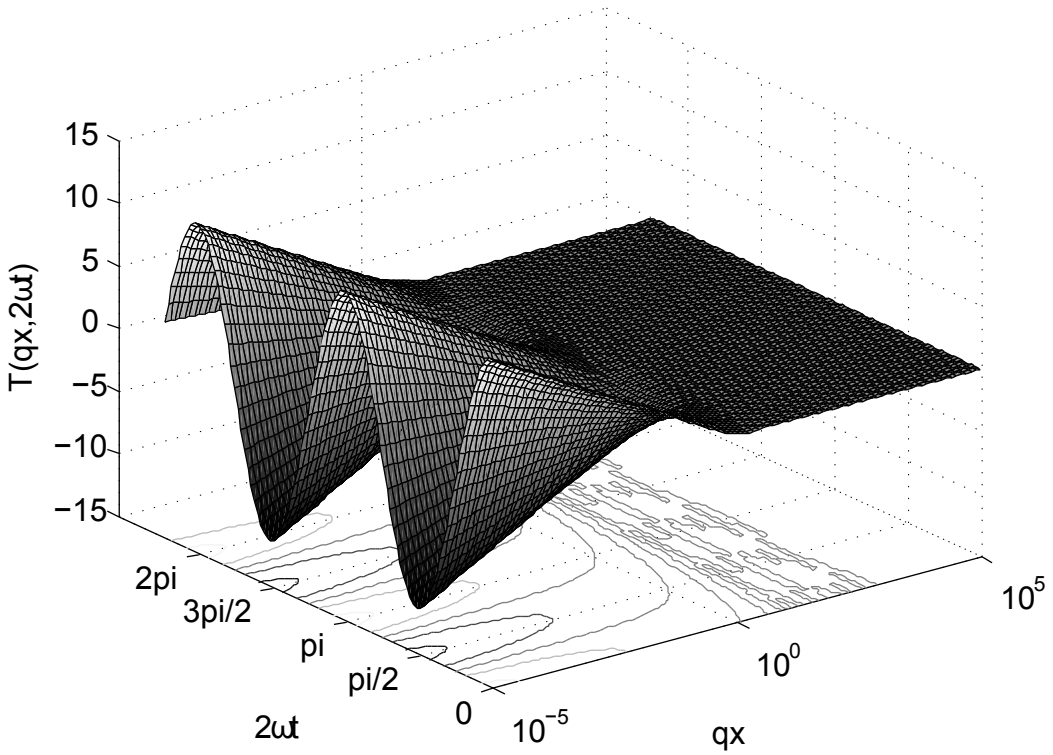

Figure 6: Visualization of the real part of equation (42). The oscillations decay rapidly away from the heater and are even in the time-domain.

2.5 Finite heater width

Further, the heater in the experiment is not infinitely narrow but has a finite width. The effect of the finite width has to be taken into account in the analysis. This is done by constructing the heater from infinite number of 1D line heaters over the width of the heater [3]. This is visualized in figure 7. Mathematically this is done by taking a Fourier transform of (41) with respect to x-coordinate. Only the oscillations at the surface are important, so $y = 0$. Now Fourier cosine transformation can be used because the temperature function is an even function. The Fourier cosine transform pair is:

$$\hat{f}(\eta) = \int_0^\infty f(x)\cos(\eta x)\mathrm{d}x, \tag{44}$$

$$f(x) = \frac{2}{\pi}\int_0^\infty \hat{f}(\eta)\cos(\eta x)\mathrm{d}\eta. \tag{45}$$

For the spatial temperature oscillations the cosine transform reads [19]

$$T(\eta) = \int_0^\infty T(x)\cos(\eta x)\mathrm{d}x = \frac{p_0}{\pi k}\int_0^\infty K_0(qx)\cos(\eta x)\mathrm{d}x = \frac{p_0}{2k}\frac{1}{\sqrt{\eta^2+q^2}}. \tag{46}$$

The finite width can be added into (46) by multiplying it with the Fourier transform of the heat source as a function of the x-coordinate. Heat enters the specimen evenly over the width of the heater ranging from $-b$ to b. This behavior can be expressed as a rectangular function with values 1 for $x < |b|$ and 0 elsewhere. According to the convolution theorem, the multiplication of the Fourier transforms of (46) and the rectangular function equals the Fourier transform of the convolution of the functions in the x-space.

$$T(\eta) = \frac{p_0}{2k}\frac{1}{\sqrt{\eta^2+q^2}}\int_0^\infty \mathrm{rect}(x)\cos(\eta x)\mathrm{d}x = \frac{p_0}{2k}\frac{\sin(\eta b)}{\eta b\sqrt{\eta^2+q^2}}. \tag{47}$$

Inverse transform gives

$$T(x) = \frac{p_0}{\pi k}\int_0^\infty \frac{\sin(\eta b)\cos(\eta x)}{\eta b\sqrt{\eta^2+q^2}}\mathrm{d}\eta. \tag{48}$$

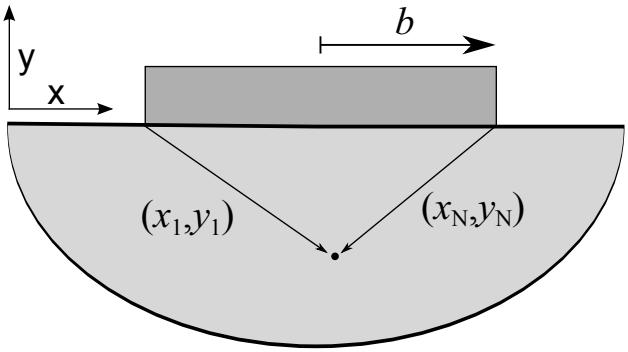

Figure 7: The temperature inside the specimen at a certain point is result of the heat flow from all the one dimensional line sources that make up a heater of finite width.

Equation (48) gives the form of temperature oscillations on the surface of the specimen a distance x away from the center of the heat source that has a finite width $2b$. Since the thermometer and the heater are the same element the measured temperature is some average temperature over the width of the line. Expression (48) can be averaged by integrating it with respect to x from 0 to b and dividing by b to give the temperature measured by the thermometer:

$$T_{avg} = \frac{1}{b}\int_0^b T(x)\mathrm{d}x = \frac{p_0}{\pi k}\int_0^\infty \frac{\sin^2(\eta b)}{(\eta b)^2\sqrt{\eta^2+q^2}}\mathrm{d}\eta. \tag{49}$$

Equation (49) is plotted in figure 8. The linear (on logarithmic scale) regime at the small frequencies is used to calculate the thermal conductivity of the specimen. The expression (49) cannot be solved in closed form, but at the limit of large thermal penetration depth an asymptotic solution exists. To deem the thermal penetration depth large it has to be compared to the heater half-width b, which is in the same length scale [3]. When the heater half-width b is much smaller than the thermal penetration depth λ, we can write

$$\lim_{b\to 0}\frac{\sin(b\eta)}{(b\eta)} = 1. \tag{50}$$

Values of η between $\lambda < \eta < 1/b$ dominate the integral and the upper limit

can be set to $1/b$ [3]. After these, the expression can be approximated as

$$T_{avg} \approx \frac{p_0}{\pi k} \int_0^{1/b} \frac{1}{\sqrt{\eta^2 + q^2}} \mathrm{d}\eta = \frac{p_0}{\pi k} \left[\ln\left(\frac{1}{b} + \sqrt{\frac{1}{b^2} + q^2} \right) - \ln q \right]$$
$$\approx \frac{p_0}{\pi k} \left(\ln 2 - \ln(qb) \right), \tag{51}$$

where series expansion for the logarithm at $b = 0$ was used in the last approximation. It is more convenient to express this in terms of the thermal excitation frequency 2ω, remembering that $q = (1 + \mathrm{i})\sqrt{\omega/\alpha}$:

$$T(2\omega) = -\frac{p_0}{2\pi k} \left(\ln(2\omega) + \ln(b^2/\alpha) - 2\ln 2 \right) - \mathrm{i}\frac{p_0}{4k}. \tag{52}$$

2.6 The effect of a thin film

The effect of the thin film on the substrate can be added to equation (52) as a thermal resistance independent of the driving frequency [20]. To ensure that the edge effects do not become significant the width of the heater should be large compared to thickness of the film being measured [21]. The boundary resistance of the film/substrate interface adds to the thermal conductivity value measured for the thin film [3]. When measuring thin film thermal conductivity the heat flow from the heater should be perpendicular and uniform through the film. The effect of the film is then

$$\Delta T_f = \frac{P_0 t}{2blk_f}, \tag{53}$$

where l is the length of the heater wire, t is the thickness of the thin film, and k_f is the thermal conductivity of the film.

The amplitude of the temperature oscillations can be expressed in measurable quantities with equation (27):

$$T(2\omega) = \frac{2V_{3\omega}}{\beta I_0 R_0}. \tag{54}$$

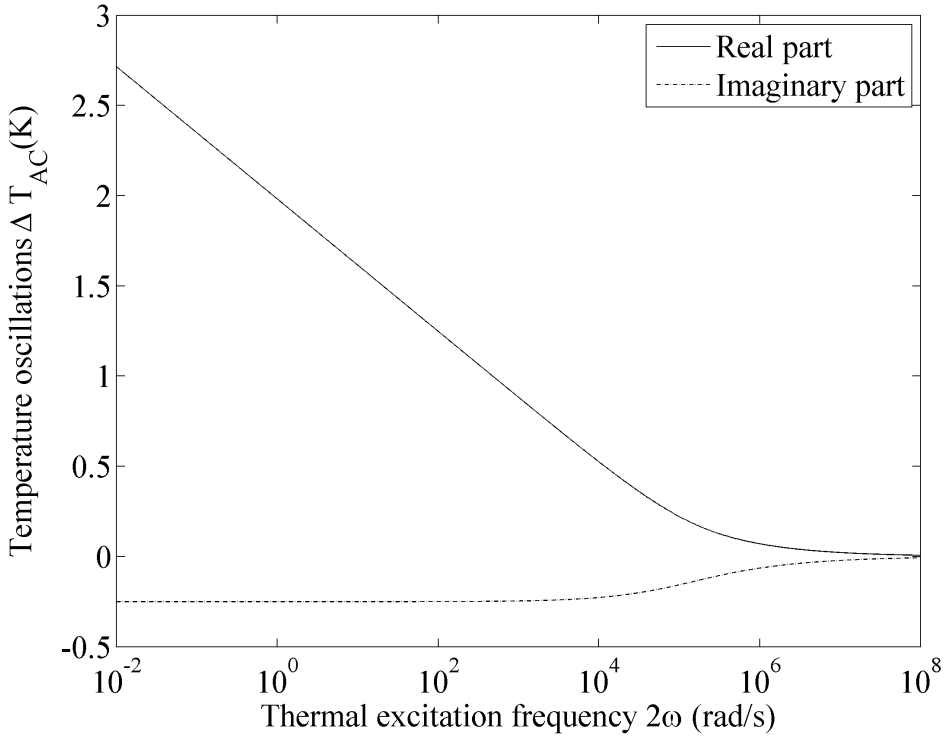

Figure 8: Visualization of equation (49). The plot shows the magnitudes of the real (in-phase) and imaginary (out-of-phase) components of the thermal oscillations versus the temperature excitation frequency 2ω. P_{rms} was set to 1 W, l to 1 m, k to 1 W/m·K, b to 5 μm and α to 1 mm^2/s.

Equations (52), (53) and (54) combine up into

$$T(2\omega) = T_s + T_f = \frac{2V_{3\omega}}{\beta I_0 R_0} = -\frac{P_0}{2\pi k_s l}\left(\ln(2\omega) + \ln(b^2/\alpha) - 2\ln 2\right) - \mathrm{i}\frac{P_0}{4k_s l} + \frac{P_0 t}{2bk_f l}, \tag{55}$$

where the subscript s denotes the substrate. Thermal conductivity of the thin film from (53) can now be expressed as

$$k_f = \frac{P_0 t}{2bl(\Delta T - \Delta T_s)}. \tag{56}$$

The thermal response of the substrate T_s can be calculated directly from equation (52) and subtracted from the measured ΔT. Thermal conductivity of the substrate can also be calculated from the slope of ΔT versus $\ln 2\omega$ as only the $\ln(2\omega)$-term has frequency dependence.

The frequency range for thin film thermal conductivity measurement depends on the applicable error level in the results when using the linear regime approximation (52). The regime can be located by monitoring the out-of-phase output, which should stay constant over the suitable frequency range. The specimen thickness should exceed 5 thermal penetration depths to contain the thermal oscillations in the sample whereas the heater half-width should be small compared to the thermal penetration depth. Also the film thickness should be small compared to the heater half-width to maintain the heat flow in 1D through the film. Applicable boundary restrictions can be set as [22]

$$5b < \lambda < t_s/5\,, \tag{57}$$

where λ is the thermal penetration depth of the substrate, introduced in subsection 2.4, and t_s is the substrate thickness. This yields for the input frequency

$$\frac{25\alpha}{4\pi t_s^2} < f < \frac{\alpha}{100\pi b^2}. \tag{58}$$

For a 800 μm thick silicon substrate with thermal diffusivity of 8.8 mm^2/s and the heater half-width of 2.5 μm the limits become

$$270\,\mathrm{Hz} < f < 45000\,\mathrm{Hz}.$$

3 Experimental Methods

3.1 Overview

Materials used in the heater fabrication for the 3ω method have included for example gold, aluminum, and silver [3, 23]. These materials have large enough temperature coefficients of resistance to create a measurable 3ω voltage signal. Gold and bismuth were used in the experiments of this work. Bismuth was chosen because the resistivity of thin films has good response to temperature changes also at low temperatures [24]. The resistivity of bulk bismuth, 1.29 μΩm, is high compared to traditional heater metals like gold with 22.14 nΩm and silver, 15.87 nΩm, all the values at 20 °C [25]. Thin bismuth films have negative TCR [24], whereas the previous studies have used heater materials with positive coefficients [3, 21, 12].

Figure 9: SEM image of a bismuth heater/thermometer deposited on SiO_x. The length of the line is 1 mm and the width is 10 μm.

3.2 Sample fabrication

The films used in the experiments were vacuum deposited on thermally oxidized boron doped silicon substrates. Oxide thickness of the films was measured with Rudolph AUTO EL III ellipsometer and found to be around 300 nm. To achieve optimal thermal contact between the heater and the substrate the chips were cleaned by sonicating them in hot acetone for $1-2$ minutes. After the sonication the chips were rinsed with isopropyl alcohol (IPA) to remove the acetone residue and blow dried with nitrogen.

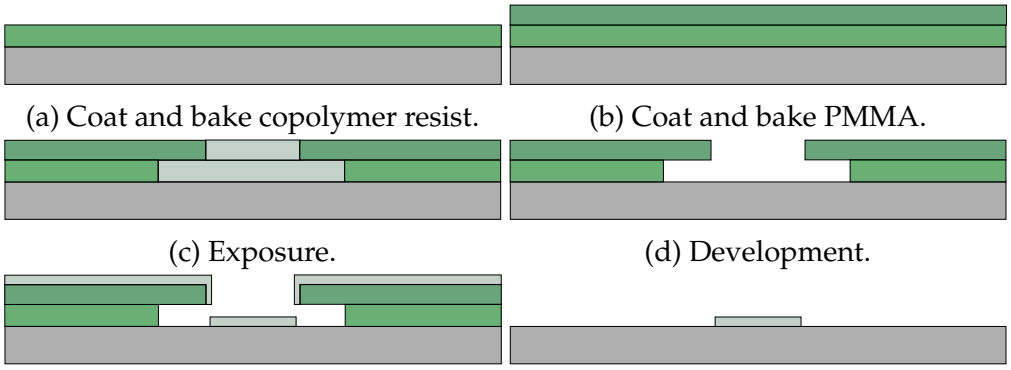

(a) Coat and bake copolymer resist. (b) Coat and bake PMMA.

(c) Exposure. (d) Development.

(e) Metal evaporation. (f) Lift-off.

Figure 10: Schematics of the lithographic process.

The sample pattern is shown in figure 9 and the lithography process in figure 10. Electron beam lithography process was used to manufacture the films. First, a copolymer resist P(MMA-MAA) EL9 or EL11 (9% or 11% polymethyl methacrylate methacrylic acid solids in ethyl lactate) is spun on the chips for 45 seconds at 2500 rpm and baked on a hot plate for 90 seconds at $\sim 160\,^{\circ}\mathrm{C}$. On top of that is spun a layer of PMMA C2 (2% solids in chlorobenzene) with the same spinning recipe and bake time. Copolymer resist is more easily exposed by the electron beam than the PMMA and creates and undercut structure. Undercut eases the lift-off step as the metal pattern is not adhered into the resist [26]. The sample pattern was designed with Elphy Quantum 1.3 software and patterned with LEO 1430 scanning electron microscope. After the exposure the top layer of the stack was developed in a mixture of methyl isobuthyl ketone (MIBK) and isopropanol alcohol (IPA) (1:2 v/v) for $\sim 30-45$ seconds, rinsed with IPA and dried

with nitrogen. The bottom layer was further developed in a 1:2 v/v mixture of 2- methoxyethanol and methanol for ~ 5 seconds, rinsed with IPA and dried in nitrogen flow.

The gold films were evaporated with a custom-made ultra-high vacuum e-beam evaporator at a rate of 2 nm/s. A 15 nm titanium layer was used as an adhesion layer for the gold heater. Bismuth was evaporated by Balzers BAE 250 vacuum e-beam evaporator at a base pressure of ~ 5 mbar. Bismuth used for the films is 99.9999% pure, obtained from Goodfellow Inc. Evaporation rate was around 2 nm/s. The lift-off was done in hot acetone, with a brief sonication if necessary. After the lift-off the chips were rinsed with IPA and dried.

3.3 Measurement setup

The schematics of the measurement setups are shown in figures 11 and 12. Stanford Research Systems SR830 lock-in amplifier is used to supply the fundamental sinusoidal heater voltage and to read the ω and 3ω signals.

In the first setup the current bias is achieved by using a load resistor R_0 in series with the sample, 10 kΩ for gold samples and 100 kΩ for bismuth. Voltage drop across the sample is measured differentially with the lock-in amplifier, both the 3ω and the fundamental 1ω voltages are measured simultaneously by using separate lock-in amplifier to read the different harmonics. The fundamental signal is fed as the reference signal to both of the lock-in amplifiers. Temperature of the sample stage is measured with a Pt100 resistance thermometer by reading its resistance with AVS resistance bridge.

The second approach involves a Wheatstone bridge to extract the 3ω voltage originating from the sample, as shown in figure 12. Resistor R_2 is one hundred times larger than R_1 to get almost all of the current pass through the sample resistance R_s. With the bridge setup it is possible to increase the resistive heating of the metal line as more current can be passed through it. The bridge is balanced by tuning the variable resistor R_v and monitoring the voltage between the bridge arms by SR830 lock-in amplifier. The 3ω output of the balanced bridge $W_{3\omega}$ is related to $V_{3\omega}$ of the sample by

$$W_{3\omega} = \frac{R_1}{R_s + R_1} V_{3\omega},$$

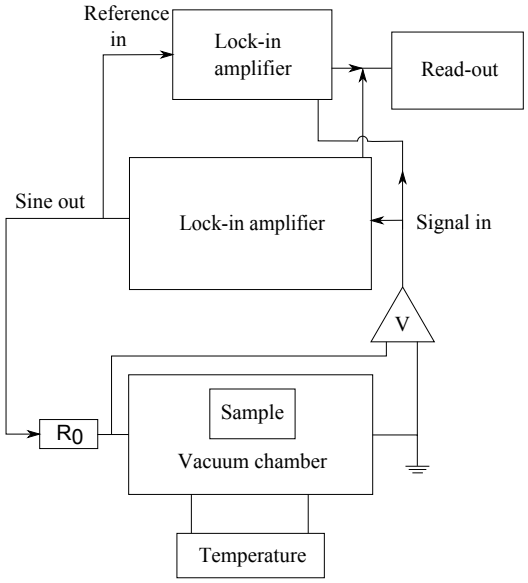

Figure 11: Schematic of the measurement setup. Two lock-in amplifiers make it possible to read the fundamental 1ω voltage and the 3ω voltage simultaneously.

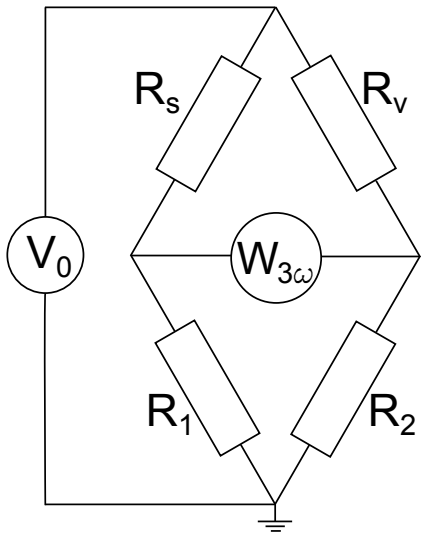

Figure 12: Schematics of the Wheatstone bridge measurement setup. SR830 lock-in amplifiers were used to supply the fundamental voltage and to read the 3ω response.

where R_s is the room temperature resistance of the sample and R_1 is the resistance of the in-series resistor [27].

3.4 Measurements

The 3ω measurements were performed at room temperature and above by using a custom compiled measurement instrumentation. A picture of the vacuum chamber, the electrical feedthrough and the sample stage is seen in figure 13. The samples were mounted on the sample stage with silver paint to ensure good thermal contact and easy removal. Electrical contacts for the gold samples were made with Kulicke & Soffa 4523A wire bonder with Al-wire. For bismuth samples the electrical contacts were made by melting a piece of indium into the tip of a wire and pressing it to the bonding pad with a scalpel tip. The bonding pads were made large for this reason. This approach is required because bismuth is a soft material and traditional ultrasonic bonding does not work properly on it. The Pt100 resistance thermometer was mounted on the stage with thermal grease to measure the temperature of the system. The sample stage was inserted

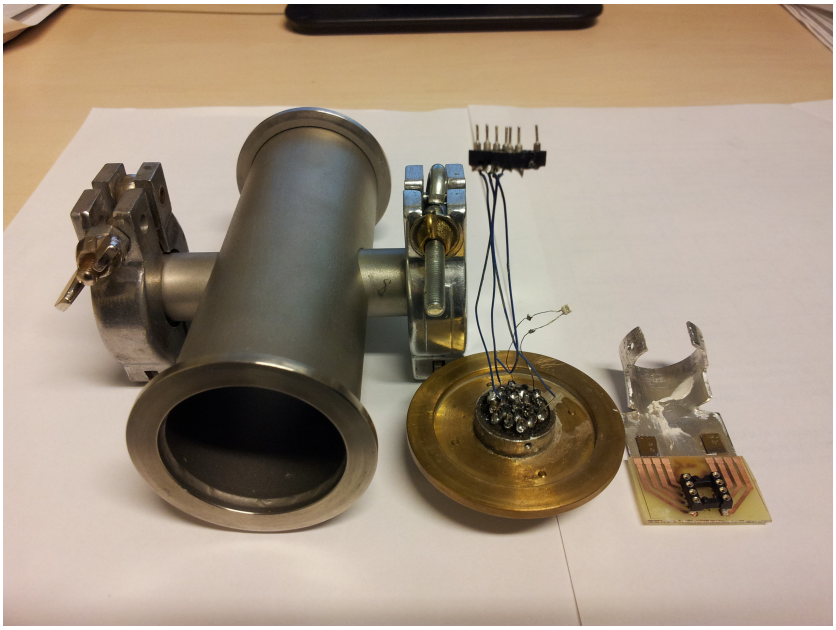

Figure 13: The vacuum chamber with the electrical feedthrough and the sample stage.

into a vacuum chamber to minimize the heat loss to the surroundings. A vacuum of $10^{-3} - 10^{-4}$ mbar was achieved with a diffusion pump.

Measurement data were collected with a custom LabVIEW virtual instrument capable of handling all the necessary input channels at the same time. The temperature coefficient of resistance of the metal line was measured prior to the 3ω measurements. The vacuum chamber was heated up to 40 °C by blowing hot air into the walls with a hot-air gun. Temperature response of the heater voltage was then measured during the cooling of the vessel back to the room temperature. Small amplitude signal of 0.1 V rms with 100 Hz frequency at lock-in output was used to avoid resistive heating of the metal line. A 100 kΩ resistor in series with the sample was used to limit the current in the circuit. Temperature of the stage was simultaneously measured with the Pt100 to fix the heater data on a temperature scale.

Actual 3ω measurements were performed at room temperature or during the cooldown after heating. Frequencies were scanned between $100 - 1000$ Hz at 100 Hz intervals with a LabVIEW instrument specially made for this purpose. Each frequency was maintained for 10 seconds to stabilize the readings. However, the requirement of the stable readings led into measurement times being over 2 minutes and the temperature of the sample stage decreased by multiple degrees during the frequency sweep from 100 to 1000 Hz. Maintaining stable temperature with the hot-air gun proved to be challenging and so the measurements were performed near the room temperature where the temperature change of the sample stage was negligible. The magnitude of the driving current was set so that the amplitude of the 1ω voltage was approximately 10000 times larger than the 3ω voltage. At this ratio the fluctuations of the output signal remained moderate so that the measurements could be performed.

The manual bonding method of the electrical contacts into bismuth samples turned out to be problematic. Most of the contacts made into the films did not survive long enough for he measurement cycles to be performed. Some contacts were lost by accidentally heating the specimen vessel too much and thus melting the indium contacts. The failing of the electrical contact between the wire and the bismuth pads was observed as increasing of the sample resistances.

4 Results

The temperature coefficient of resistance of the metal heater was obtained by linear regression from the measured temperature response. For bismuth an example is shown in figure 14 and for gold in figure 15. Resistance of the heater was obtained from the fundamental 1ω voltage measured over the heater. The value of the TCR is obtained by dividing the slope of the temperature response of the metal line with the heater resistance at ambient temperature. For bismuth lines the TCR values are around $2 \cdot 10^{-3}$ 1/K and for gold lines around $3 \cdot 10^{-3}$ 1/K.

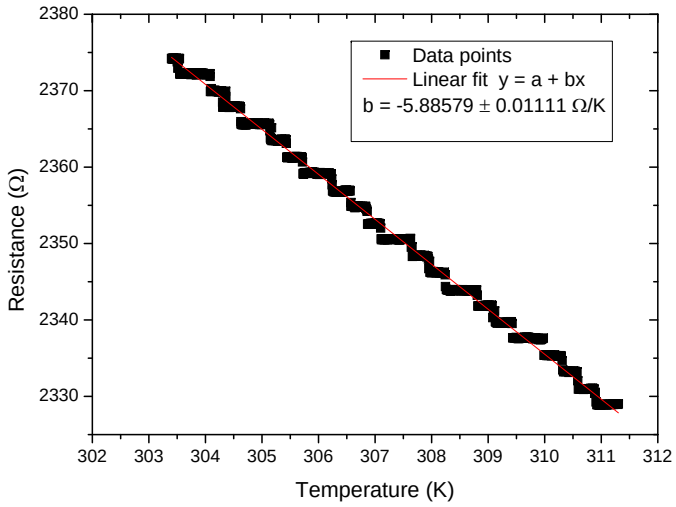

Figure 14: Resistance of a 5 μm wide and 300 nm thick bismuth line versus temperature near the room temperature. Step-like behavior is due to insufficient resolution.

The error in the temperature oscillations of the specimen builds up mostly from the error in TCR measurement and the fluctuations in the output of the 3ω voltage. Possible error sources can be seen in equation (54), $V_{3\omega}$ and the TCR dominate the error. The linear fit into heater data for TCR is accurate, some error may arise from the lag between the heater and the Pt100 sensor. If the response time of the Pt100 is multiple seconds

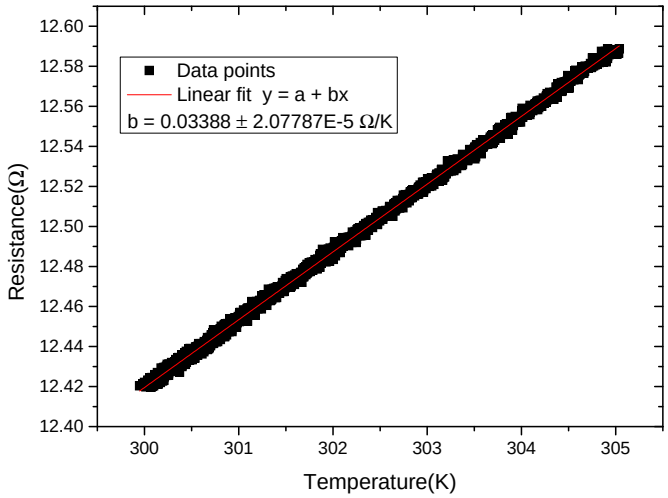

Figure 15: Resistance of a 10 μm wide and 250 nm thick gold line versus temperature near the room temperature.

behind that of the metal line the temperature scale of the linear fit is off by some degrees. The measured temperature response of the metal lines is however linear over a range of 10 degrees so a lag of some degrees would not affect the value of TCR.

Measured 3ω voltages for a 5 μm wide and 300 nm thick bismuth heater are seen in table 1. Temperature oscillations in the substrate are calculated from equation (52). Values used for thermal conductivity and thermal diffusivity of the silicon substrate are 149 W/m·K and $8.8 \cdot 10^{-5}$ m^2/s, respectively [25]. The values measured with the setup of figure 11 are seen in table 1 along the results for the measured temperature oscillations, the measured temperature oscillations in the thin film and the calculated thermal conductivity of the film. The thermal conductivity of the silicon dioxide film is calculated with equation (56), the film thickness set to 300 nm. Results for a 10 μm wide and 250 nm thick gold heater measured with the setup of figure 11 are seen in table 2.

The calculated values for temperature oscillations in the substrate are small when compared into values reported earlier [23, 20]. The oscillations

Table 1: Output data for a 5 μm wide and 300 nm thick bismuth heater. The driving frequency and the corresponding temperature oscillations of the whole specimen, the film, and the substrate plus the thermal conductivity of the thin film. Measurement was done with 0.75 V input voltage to get a well reacting 3ω output. The heater power per unit length is 121 μW/m.

f (Hz)	$V_{3\omega}$ (μV)	ΔT (K)	ΔT_s (μK)	ΔT_f (K)	k_f (W/m·K $\cdot 10^{-5}$)
100	2.77	0.140	1.52	0.140	5.18
200	2.80	0.142	1.42	0.142	5.13
300	2.79	0.141	1.37	0.141	5.14
400	2.81	0.142	1.33	0.142	5.11
500	2.81	0.142	1.30	0.142	5.12
600	2.84	0.144	1.27	0.144	5.06
700	2.85	0.144	1.25	0.144	5.05
800	2.89	0.146	1.24	0.146	4.98
900	2.88	0.145	1.22	0.145	5.01
1000	2.88	0.145	1.21	0.145	5.01

Table 2: Output data for a 10 μm wide and 250 nm thick gold heater. The driving frequency and the corresponding temperature oscillations of the whole specimen, the film, and the substrate plus the thermal conductivity of the thin film. Measurement was done with 3.156 V input voltage to get a well reacting 3ω output. The heater power per unit length is 1.4 mW/m.

f (Hz)	$V_{3\omega}$ (μV)	ΔT (K)	ΔT_s (μK)	ΔT_f (K)	k_f (W/m·K $\cdot 10^{-5}$)
100	4.26	0.703	16.8	0.703	5.98
200	4.21	0.693	15.6	0.693	6.06
300	4.23	0.697	14.9	0.697	6.02
400	4.21	0.694	14.4	0.694	6.05
500	4.24	0.699	14.0	0.699	6.00
600	4.25	0.701	13.7	0.701	5.99
700	4.25	0.700	13.4	0.700	6.00
800	4.22	0.695	13.2	0.695	6.04
900	4.23	0.698	13.0	0.698	6.02
1000	4.31	0.710	12.8	0.710	5.91

in the substrate should be of the same order of magnitude as the total oscillations. The error in the measurement causes the calculated thermal conductivity of the silicon dioxide film to be 5 orders of magnitude off from an acceptable value about 1.3 W/m·K [23, 20]. The expected 3ω output of the measurement can be calculated when the film thermal conductivity is fixed to 1.3 W/m·K. The values obtained from equation (55) give values around $1 - 2 \cdot 10^{-10}$ V. Measurements performed with the Wheatstone bridge setup were unsuccessful. The circuit did not give reasonable readings for the 3ω voltage over the bridge. This is probably due to third harmonic noise from the components or the signal sources that were used in the setup.

The vacuum does not affect the output value of the 3ω signal. This is not desired behavior as the heat generated in the metal line should be conducted into the surrounding air when measuring in atmospheric pressure. The reason behind this is probably the noise in the circuit. The out-of-phase signal, which can be used to locate the linear regime [3], did not show any linear behavior. The signal was however smaller than the in-phase signal by a factor of ten, which is somewhat proper behavior. Fluctuations in both the magnitude and the phase of the out-of-phase signal were unpredictable and the identification of the linear regime based on the out-of-phase output proved implausible.

5 Conclusions and Future Work

The goal of validation of the 3ω method for thermal conductivity measurements was not achieved. Obtained 3ω signal did not contain information about the thermal properties of the measured samples. At first this was thought to be due to low power level in the metal line heater, but further measurements with the Wheatstone bridge setup suggest that the cause is spurious 3ω signals from the components. The actual source of this signal remains unknown.

If the 3ω measurements are further pursued the measurement setup should be rebuilt keeping in mind the requirement of accurate temperature control of the stage and high enough power in the metal line heater. For temperatures lower than room temperature a dipstick with vacuum would be optimal. Raising the dipstick from liquid helium or liquid nitrogen provides slow and controllable rate of temperature change and accurate measurements at precise temperatures would be possible. A standardized specimen mount with connections to the dipstick would ease the problems with the electrical connections to the sample.

A more sophisticated LabVIEW instrument to sweep frequencies at smaller intervals than 100 Hz would ease the locating of the linear regime. At one frequency step the instrument should record the in-phase 1ω and 3ω voltages over the sample plus the out-of-phase 3ω signal with the phase lag. For SR830 GPIB bus can be used to command the lock-in amplifier to change the signal frequency and the channel output. A possible problem may arise from the lock-in amplifier's limited output signal magnitude. A common multimeter can be used to monitor the 1ω voltage if the output range of the lock-in amplifier is exceeded. Temperature measurements below $-200\,^{\circ}\mathrm{C}$ require a temperature probe other than Pt100.

References

[1] D.G. Cahill et al., J. Appl. Phys. 93 (2003) 793.

[2] W.S. Capinski et al., Phys. Rev. B 59 (1999) 8105.

[3] D.G. Cahill, Rev. Sci. Instrum. 61 (1990) 802.

[4] O.M. Corbino, Phys. Z. 11 (1910) 413.

[5] O.M. Corbino, Phys. Z. 12 (1911) 292.

[6] L.R. Holland, J. Appl. Phys. 34 (1963) 2350.

[7] D. Gerlich, B. Abeles and R.E. Miller, J. Appl. Phys. 36 (1965) 76.

[8] L.R. Holland and R.C. Smith, J. Appl. Phys. 37 (1966) 4528.

[9] N.O. Birge and S.R. Nagel, Phys. Rev. Lett. 54 (1985) 2674.

[10] N.O. Birge and S.R. Nagel, Rev. Sci. Instrum. 58 (1987) 1464.

[11] D.G. Cahill and R.O. Pohl, Phys. Rev. B 35 (1987) 4067.

[12] S.M. Lee, D.G. Cahill and T.H. Allen, Phys. Rev. B 52 (1995) 253.

[13] G. Gesele et al., J. Phys. D 30 (1997) 2911.

[14] X.J. Hu et al., J. Heat Transfer 128 (2006) 1109.

[15] H. Carslaw and J. Jaeger, Conduction of heat in solids (Clarendon Press, 1959).

[16] K. Banerjee et al., Reliability Physics Symposium Proceedings, 1999. 37th Annual. 1999 IEEE International, pp. 297 –302, 1999.

[17] U.G. Jonsson and O. Andersson, Meas. Sci. Technol. 9 (1998) 1873.

[18] N.O. Birge, Phys. Rev. B 34 (1986) 1631.

[19] A. Erdélyi, Tables of Integral Transforms (McGraw-Hill, 1954).

[20] S.M. Lee and D.G. Cahill, J. Appl. Phys. 81 (1997) 2590.

[21] D.G. Cahill, M. Katiyar and J.R. Abelson, Phys. Rev. B 50 (1994) 6077.

[22] D. de Koninck, Thermal conductivity measurements using the 3-omega technique: Application to power harvesting microsystems, Master's thesis, Department of Mechanical Engineering, McGill University, Montréal, Canada, 2008.

[23] T. Yamane et al., J. Appl. Phys. 91 (2002) 9772.

[24] R.A. Hoffman and D.R. Frankl, Phys. Rev. B 3 (1971) 1825.

[25] W. Haynes and D. Lide, CRC Handbook of Chemistry and Physics: A Ready-Reference Book of Chemical and Physical Data .

[26] MicroChem PMMA Data Sheet, `http://microchem.com/pdf/PMMA_Data_Sheet.pdf`, Accessed 12/2012.

[27] N.O. Birge, P.K. Dixon and N. Menon, Thermochim. Acta 304–305 (1997) 51 .